Revisiting the Influence of Dispersive Characteristics of Soil Electrical Parameters on Transient Behavior of Underground Cables: Impacts on Wave Propagation and Practical Case Studies

Rafael Alipio, Naiara Duarte, Alberto De Conti

***Abstract*-- This paper revisits the influence of the frequency dependence of electrical soil parameters on the simulation of electromagnetic transients in underground insulated cables. The analysis shows that this effect is particularly pronounced for short cable sections and soils with resistivities higher than 1000 Ωm, resulting in non-negligible differences in simulated transient overvoltages when compared to models assuming constant soil parameters. These differences affect both the amplitude and the waveform of the overvoltages. Furthermore, results from two illustrative case studies highlight that the magnitude of this effect depends on the specific system configuration and the type of transient phenomena under study, emphasizing the importance of accounting for it. The findings underscore the necessity of considering the frequency dependence of soil parameters in transient studies where highly accurate results are required.**

***Keywords*: Dispersive soil characteristics; ground-return parameters; high-frequency transients; soil modeling; underground cables.**

I. INTRODUCTION

IN recent years, the topic of underground insulated cable modeling has gained significant attention from the electromagnetic transient (EMT) community, with focus on developing accurate expressions, or approximations of these, to compute the ground-return impedance and admittance for transmission line theory simulations [1-7], and on validating the limits of such expressions using full-wave methods [8], [9]. These recent studies not only addressed an important scientific gap in the field but also played a key role on increasing the accuracy in the simulation of electromagnetic transients in underground cable systems, which are increasingly present in electrical networks, notably in renewable energy plants [10]. For instance, in wind parks and photovoltaic farms, it is common to have collector systems composed of underground cables directly buried in the ground, which makes the accurate computation of ground effects even more critical. Another example is the use of short underground cable sections in hybrid overhead-underground lines [11,12] and at the entry points of gas-insulated (GIS) substations, further emphasizing the relevance of accurate ground effect computations [13].

Over the last decade, research has also been conducted to characterize the frequency dependence of electrical soil parameters (a summary can be found in [14]), namely conductivity and permittivity, which exhibit substantial variation from DC to a few MHz. The initial focus of these studies was to assess the impact of the frequency dependence of soil parameters on grounding system performance [15], [16]. Later, this scope was expanded to include the study of induced voltages from nearby lightning strikes [17,18] and overhead line modeling [19,20]. As a natural progression, recent works have evaluated the influence of dispersive soil parameters in the simulation of transients in underground cables, adopting distinct formulations for calculating the ground-return impedance and admittance, as well as different approaches to incorporate the frequency-dependent behavior of conductivity and permittivity [21-23]. A fundamental work on the impact of soil frequency dependence in cable systems was conducted in [22] and later extended to different cable configurations in [24]. Additionally, [22] presents a step-by-step procedure and frequency-based criteria for evaluating the influence of soil modeling, the formulation of ground-return parameters, and section length in underground cable systems. A common conclusion of these studies is that considering frequency-dependent soil parameters can change the high-frequency content of transient phenomena in underground cables, particularly in poorly conducting soils. However, these studies do not fully establish the extent to which this effect should be incorporated or its relative importance in insulation coordination studies.

The main objective of this work is to complement previous studies and revisit the influence of frequency-dependent (FD) electrical soil parameters on the simulation of electromagnetic transients in underground insulated cables. The key additions and contributions of this study, compared to prior works, are summarized as follows.

This paper was financed in part by the National Council for Scientific and Technological Development (CNPq) (304157/2022-8, 406177/2021-0 and 314849/2021-1), and in part by the Coordenação de Aperfeiçoamento de Pessoal de Nível Superior - Brasil (CAPES).

R. Alipio and N. Duarte are with the Department of Electrical Engineering, Federal Center of Technological Education (CEFET-MG), Belo Horizonte, MG, 30510-000, Brazil (emails: rafael.alipio@cefetmg.br and naiara.duarte@gmail.com).

A. De Conti is with the Department of Electrical Engineering, Universidade Federal de Minas Gerais (UFMG), Belo Horizonte, MG, 31270-901, Brazil (e-mail: conti@cpdee.ufmg.br).

Paper submitted to the International Conference on Power Systems Transients (IPST2025) in Guadalajara, Mexico, June 8-12, 2025.

First, the frequency dependence of the soil electrical parameters is modeled using the Alipio-Visacro model [25], which is recommended by the CIGRE for studies involving lightning transients [14]. As shown in [25], this model is suggested to better represent the frequency dependence of soil parameters in cases of poorly conducting soils, precisely the situation where this phenomenon's influence is most significant. Consequently, the analysis in this paper is extended to high-resistivity soils (up to 5000 Ωm), aiming to clarify the impacts of the frequency dependence of soil parameters that are not apparent in high-conductivity soils. Second, two illustrative case studies are discussed: one involving high-frequency transients in an underground cable section of a hybrid overhead-underground line, and another examining a wind turbine struck by lightning. These cases aim to provide further insights into practical scenarios where the frequency dependence of soil parameters may significantly impact the simulation of transients in underground cable systems, while also contributing to the clarification of this effect and paving the way for its incorporation into EMT-type simulation platforms.

II. System Under Study and Modeling

A flat cable system configuration is considered in this paper, as shown in Fig. 1(a). The cables are buried at a depth h=1 m with a spacing x_{ij}=0.3 m. The cables are single core with a conducting sheath. Each cable is modeled according to the data presented in Table I considering the cross-section shown in Fig.1(b).

The matrices corresponding to the per-unit-length impedance $\boldsymbol{Z}$ and admittance $\boldsymbol{Y}$ of an underground cable system are given by

$$\boldsymbol{Z} = \boldsymbol{Z_i} + \boldsymbol{Z_e} \tag{1}$$
$$\boldsymbol{Y} = (\boldsymbol{Y_i}^{-1} + \boldsymbol{Y_e}^{-1})^{-1} \tag{2}$$

where $\boldsymbol{Z_i}$ and $\boldsymbol{Y_i}$ are the internal impedance and admittance matrices, respectively, and can be calculated as indicated in [26]. The external impedance and admittance matrices, $\boldsymbol{Z_e}$ and $\boldsymbol{Y_e}$, respectively, are related to the ground-return parameters. In this paper, these matrices are computed using the generalized formulation proposed by Xue *et al.* [4]. The accuracy of this formulation was evaluated through comparisons with a full-wave FDTD code [8], [9], as well as more recently with experimental results derived from the transient response of a single coated wire [27].

For representing the dispersive characteristic of the soil electrical parameters, the soil model proposed by Alipio and Visacro is adopted [25]. This model is based on the measurement of the frequency response of different types of soils in natural conditions, including several high-resistivity soils where the effect of the dispersive characteristic is significant. For the constant soil parameter hypothesis, which is considered in this paper for comparison purposes, the soil is characterized by its conductivity σ_g and a relative permittivity ε_{rg}=10, both assumed frequency-independent. In all cases, the permeability of the soil is assumed constant and equal to the vacuum permeability.

It is worth mentioning that both the formulations used in this paper to compute the ground-return parameters of the cable and the frequency variation of soil parameters present experimental validation [25], [27].

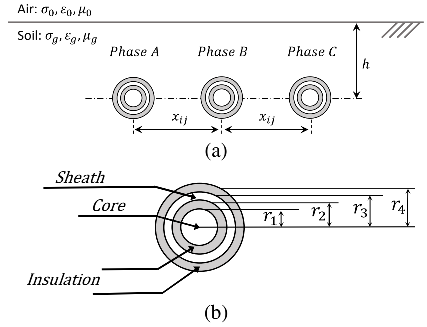

Fig. 1. Simulated system: (a) flat arrangement and (b) underground cable cross-section.

TABLE I
SINGLE-CORE CABLE DATA

Core radius r_1	0.0234 m
Inner insulation radius r_2	0.0385 m
Sheath radius r_3	0.0413 m
Outer insulation radius r_4	0.0484 m
Core resistivity	1.7×10^{-8} Ωm
Lead sheath resistivity	2.1×10^{-8} Ωm
Inner insulation relative permittivity	3.5
Outer insulation relative permittivity	2.3
All relative permeabilities	1.0

III. Wave Propagation Characteristics

To assess the influence of FD soil parameters on the wave propagation characteristics of underground cables, the modal propagation characteristics of the cable system depicted in Fig. 1(a) are considered. The attenuation constant and phase velocity of both ground-return mode and inter-sheath mode were analyzed. These modes were chosen as they are most strongly influenced by the ground-return parameters of the cable system. In the following analysis, only the results obtained for the ground-return mode are presented, as conclusions drawn for this mode are also valid for the inter-sheath mode.

Fig. 2 shows the ratio between the modal attenuation constants computed while neglecting or considering the dispersive characteristic of soil parameters, assuming resistivities of 200, 1000 and 5000 Ωm. The ratio was calculated as $\alpha = \frac{\alpha_{CP}}{\alpha_{FD}}$, where α_{CP} and α_{FD} are the attenuation constants calculated with constant (CP) and frequency-dependent (FD) soil parameters, respectively. It is observed that the attenuation constants are identical up to a critical frequency f_1, which decreases as the soil resistivity increases. Above this critical frequency, the attenuation constants calculated for the FD soil show a reduction compared to the CP cases, especially for poorly conducting soils, resulting in $\alpha > 1$. At higher frequencies, above another critical frequency f_2, which is lower for high-resistivity soils, this behavior is inverted, that is, $\alpha < 1$. This means that the attenuation is greater for the FD soil. Furthermore, Fig. 2

illustrates that the maximum value of α increases—and shifts toward lower frequencies—as the soil resistivity increases.

Fig. 3 shows the modal phase velocities computed while neglecting or considering the dispersive characteristic of the soil parameters. The ratio was calculated as $v_f = \frac{v_{fCP}}{v_{fFD}}$, where v_{fCP} and v_{fFD} are the phase velocities calculated with CP and FD soil parameters, respectively. It is evident that the phase velocities remain identical up to a certain frequency, beyond which they become lower when the dispersive characteristic of the soil is considered. Additionally, the differences between the estimated velocities, when considering and neglecting the dispersive characteristic of the soil, are more pronounced and appear at lower frequencies in high-resistivity soils.

A similar analysis on the effect of ground admittance and soil frequency dependence on cable ground-return mode propagation was previously conducted by Papadopoulos *et al.* in [22], considering the ground-return parameters computed using the formulation proposed in [1] and that of Smith and Longmire for FD soil modeling [14]. Assuming soil resistivities of 100 Ωm and 1000 Ωm, analogous results to those reported in this section were obtained in [22] for both the attenuation constant and phase velocity. The magnitude of the observed differences between constant and FD soil parameter assumptions in the propagation characteristics was also comparable to those shown in Figs. 2(a) and (b) and Figs. 3(a) and (b), respectively. However, in this study, which employs the Alipio-Visacro model for FD soil computation, the differences for the 1000-Ωm soil are slightly more pronounced.

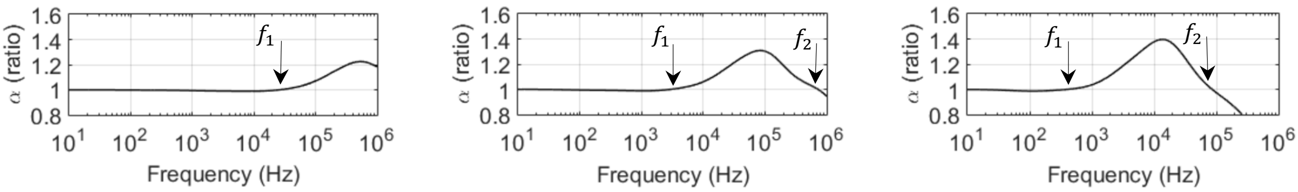

(a) (b) (c)

Fig. 2. Ratio between the modal attenuation constant for ground-return mode calculated as $\alpha = \alpha_{CP}/\alpha_{FD}$, where α_{CP} and α_{FD} are the attenuation constants obtained using constant and frequency-dependent soil parameters for different soil resistivities: (a) 200 Ωm, (b) 1000 Ωm and (c) 5000 Ωm, considering the flat arrangement depicted in Fig. 1.

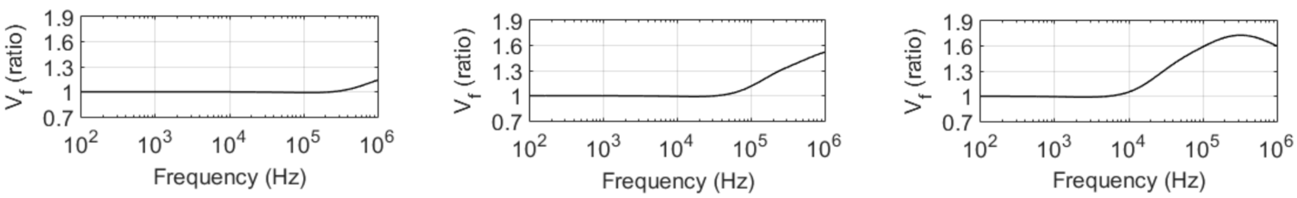

(a) (b) (c)

Fig. 3. Ratio between the modal phase velocity for ground-return mode calculated $v_f = v_{fCP}/v_{fFD}$, where v_{fCP} and v_{fFD} are the phase velocities obtained using constant and frequency-dependent soil parameters for different soil resistivities: (a) 200 Ωm, (b) 1000 Ωm and (c) 5000 Ωm, considering the flat arrangement depicted in Fig. 1.

IV. Transient Response

In this section, the transient response of the cable system of Fig. 1(a) is analyzed under ground-return mode excitation. This response is calculated using the nodal admittance matrix, derived from the exact frequency-domain solution of the telegrapher's equations [28]. All calculations are performed in the frequency domain, and the time-domain response is obtained via the numerical inverse Laplace transform [29]. As shown in Fig. 4, one terminal of the unit-step voltage source is connected to the short-circuited sending ends of the sheaths, while the other is grounded. The receiving ends of the sheaths, along with all core ends, are left open. The results are shown in Figs. 5 and 6 for cable lengths of 100 m and 500 m, respectively, and soil resistivities of 200, 1000, and 5000 Ωm.

The voltage waveforms in Figs. 5 and 6 show that increasing soil resistivity reduces sheath voltages at the receiving end of the cable for ground-return mode excitation. This effect is due to the increase of both α_{CP} and α_{FD} as the ground becomes less conductive, leading to greater attenuation of propagating voltage waves. However, these parameters increase at different rates, as indicated by the increase in the α_{CP}/α_{FD} ratio in the f_1-f_2 range shown in Fig. 2. For a soil resistivity of 200 Ωm, the variation in the α_{CP}/α_{FD} ratio only becomes significant above approximately 100 kHz, which is insufficient to affect the sheath voltages. This leads to a behavior that is practically insensitive to the soil model.

As soil resistivity increases, the frequency band defined by f_1 and f_2 gradually shifts toward lower frequencies, and the α_{CP}/α_{FD} ratio progressively increases, impacting frequency components of the propagating surge in the range of a few kHz to tens of kHz. Consequently, sheath voltages calculated with the dispersive soil model are likely to be higher than those calculated with a constant-parameter soil, especially for shorter cables and higher-resistivity soils. For the 100-m cable and the 5000-Ωm soil, for example, the dispersive soil model yields a peak voltage nearly 20% higher than that obtained with the constant-parameter soil.

Another interesting feature observed in Figs. 5 and 6 is related to the increase in the v_{fCP}/v_{fFD} ratio shown in Fig. 3

with increasing frequency and soil resistivity. This increase implies that sheath voltages are likely to travel faster in constant-parameter soil than in dispersive soil. For the 5000-Ωm soil, this effect is evident in Figs. 5(c) and 6(c) and may negatively affect traveling-wave-based fault location techniques, resulting in larger location errors. However, for soil resistivities of 200 and 1000 Ωm, the differences in wave arrival times are less significant.

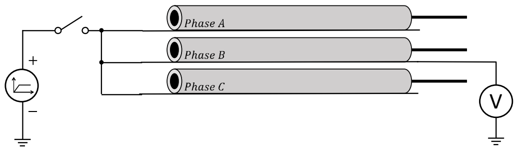

Fig. 4. Ground-return mode energization of the simulated cable system.

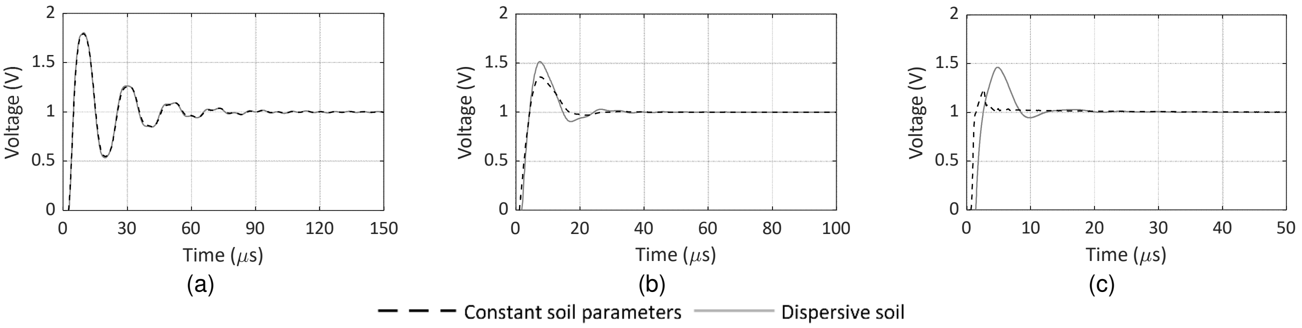

Fig. 5. Sheath voltage waveforms calculated at the receiving end of phase B, for ground-return mode energization and different soil resistivities: (a) 200 Ωm, (b) 1000 Ωm and (c) 5000 Ωm, considering constant soil parameters and dispersive soil for a flat arrangement with a total length cable of 100 m.

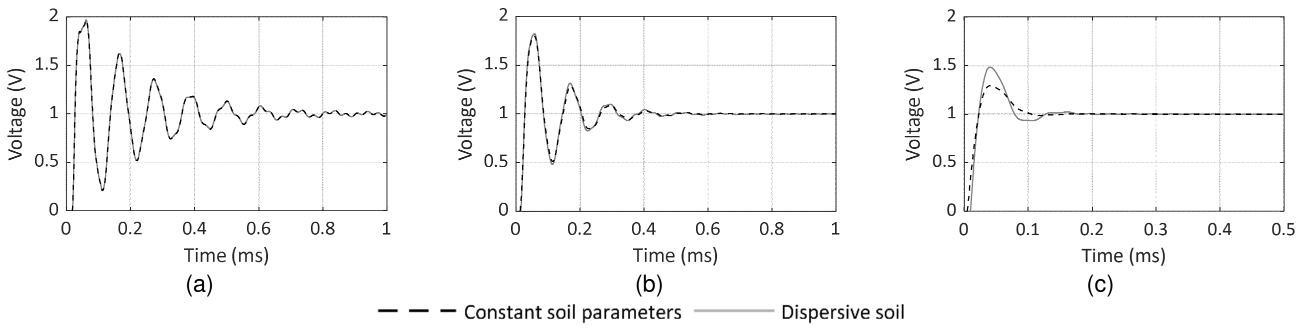

Fig. 6. Sheath voltage waveforms calculated at the receiving end of phase B, for ground-return mode energization and different soil resistivities: (a) 200 Ωm, (b) 1000 Ωm and (c) 5000 Ωm, considering constant soil parameters and dispersive soil for a flat arrangement with a total length cable of 500 m.

According to the transmission line theory, the natural frequencies associated with wave reflections at the cable ends are inversely proportional to cable length, with the fundamental frequency given by $f_0 = v/(4\ell)$, where v is the phase velocity (associated herein with the ground-return mode) and ℓ is the cable length. As the cable length increases, f_0 decreases proportionally, potentially falling below the f_1-f_2 range shown in Fig. 2. Consequently, for longer cables, the influence of the soil model on sheath voltage characterization becomes progressively less significant, as observed in Figs. 5 and 6.

The conclusions extracted from Figs. 5 and 6 are in line with the observations made by Papadopoulos *et al.* [22] adopting the formulation of Smith and Longmire to compute ground conductivity and permittivity. Similar findings were reported in [22], namely that the influence of FD soil parameters becomes more pronounced for poorly conductive soils and short cables. Furthermore, [22] proposes guidelines for selecting a consistent approach to transient analysis of underground cable systems, based on three critical frequencies. These frequencies serve as criteria for assessing whether ground admittance and FD soil modeling should be included in transient studies. As cable length increases, the spectral content of transients shifts to lower frequencies, reducing the relevance of these effects and influencing the decision to account for them. Specifically, the proposed frequency threshold, above which the frequency dependence of soil properties should be considered, is defined as the point where the deviation in σ_{FD}/σ_{DC} exceeds 10%, where σ_{FD} represents the frequency-dependent soil conductivity, while σ_{DC} corresponds to the DC or low-frequency conductivity. Although this frequency selection criterion was established using the Smith-Longmire formulation, it can be considered general and applicable to the Alipio-Visacro FD soil model.

V. Case Studies

A. Overvoltages in Mixed Overhead-Underground Cable Lines

Studying lightning overvoltages in mixed overhead-underground cable lines is critical. In the event of a backflashover across the overhead (OH) line insulators, surge voltages may propagate directly into the underground cable. In short cable sections, multiple reflections can rapidly escalate into severe overvoltages. Fig. 8 illustrates the cable configuration considered in this case study, adapted from [30]. The cable system is assumed to have the same geometrical characteristics depicted in Fig. 1. A standard lightning impulse voltage of 1 kV, 1.2/50 μs is applied at the sending end of the core of phase A, representing a transferred surge voltage into the underground cable section due to a lightning strike on an OH line. In a simplified and conservative approach, the cable cores were left open at the receiving end of the cable. The cable length is assumed to be 100 m. At the transition point between the OH line and the underground section (left end of the cable system), the sheaths are connected to the OH line grounding system, which consists of four counterpoise copper wires, each 60 m long, as illustrated in Fig. 9. At the receiving end of the underground section, the cable sheaths are bonded to the substation grounding grid, which is a square grid of 60 m × 60 m with meshes of 5 m × 5 m, as shown in Fig. 9. In the simulations presented in this section, the frequency-dependent behavior of both the OH line grounding system, $Z_{OHTL}(j\omega)$, and the substation grounding grid, $Z_{grid}(j\omega)$, was determined using an accurate electromagnetic model [30,31], and included in the nodal admittance matrix. Given the rather short distance between the transmission line grounding and the substation grounding, the same soil properties were assumed for their modeling, as well as for the calculation of the ground-return impedance and admittance of the interconnecting cable.

It is worth noting that the proposed simulation includes certain simplifications. In the scenario of a backflashover occurring in the overhead line, the resulting voltage at the cable sheath is influenced by two main factors: (i) the ground potential rise due to the lightning current flowing through the overhead line grounding system and (ii) the induced voltage caused by the current directly flowing through the cable core. The simulation accounts for the latter contribution. The results presented in Section IV, which considers a ground-return mode energization of the simulated cable system, provide some insight into the expected voltage response at the cable sheath when a surge is directly applied to the sheath. These results indicate that incorporating the frequency dependence of soil parameters in cable modeling leads to higher sheath voltages compared to assuming constant soil parameters.

This section focuses on the effect of FD soil parameters on the transient response of buried components, notably grounding systems and underground cables. The impact of FD soil parameters on surge propagation in overhead lines has been investigated in [19,20], showing that their influence is generally minor, affecting mostly voltages induced due to conductor coupling in case of very high-resistivity soils.

Fig. 10 shows the voltages calculated at the receiving end of the phase C sheath for soil resistivities of 200, 1000, and 5000 Ωm, assuming an ideal voltage source with internal impedance $Z_S = 0$ connected at the sending end of the core of phase A. Three different hypotheses are considered in the simulations: (i) Constant soil parameter assumption applied to both grounding and cable system modeling (labeled as "grounding and cable CS" – red curves); (ii) FD soil parameters in grounding modeling and constant soil parameters in cable modeling (labeled as "grounding FDS and cable CS" – black dotted curves). (iii) FD soil parameters in both grounding and cable modeling (labeled as "grounding and cable FDS" – gray curves).

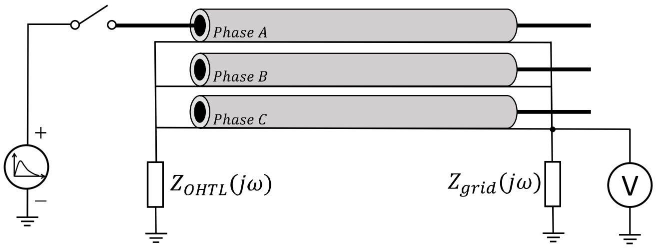

Fig. 8. Cable system subjected to a standard lightning impulse voltage of 1 kV, 1.2/50 μs, applied to the sending end of the core of phase A.

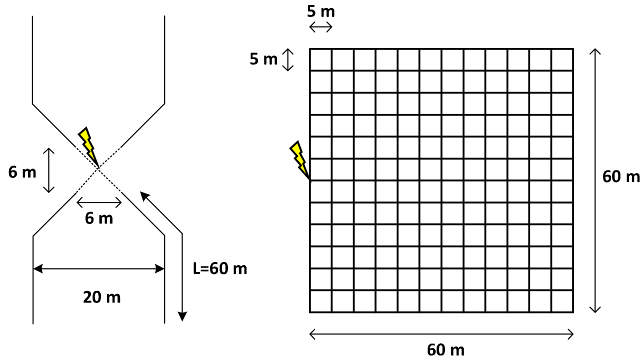

Fig. 9. Configuration of grounding systems: transmission line grounding system (left), and substation grounding grid (right). Adapted from [30].

By analyzing the simulated voltage waveforms, it is observed that accounting for the frequency dependence of soil parameters in grounding modeling (comparing the red and black dotted curves) leads to a decrease in voltage amplitude, which becomes more pronounced as soil resistivity increases. This effect stems from the improved performance of grounding systems when FD soil parameters are considered, as detailed in [15]. Comparing the gray and black dotted curves, it can be seen that considering the frequency dependence of soil parameters in cable modeling also influences simulated voltages. According to the results, incorporating FD soil parameters in cable modeling results in higher voltage amplitudes and slower wave propagation compared to assuming constant parameters. The observed differences are more significant for high-resistivity soils, although they are also noticeable for the 200-Ωm soil.

It is interesting to note that for soil resistivities of 200 Ωm and 1000 Ωm, considering FD soil parameters in grounding and cable modeling results in similar effects in terms of modifying the magnitude of the simulated voltages, but in opposite directions. Specifically, FD soil parameters lead to a reduction in voltage when incorporated into grounding modeling, whereas they cause an increase in voltage when included in cable modeling. In the case of 5000-Ωm soil, the influence of FD soil parameters in grounding modeling becomes significantly more relevant.

A notable outcome of these results is that including the frequency dependence of soil parameters in cable modeling leads to higher voltage amplitudes. At first glance, this result may seem unexpected, as the FD soil assumption leads to a decrease in soil resistivity with frequency. However, this can be explained by the fact that the attenuation constant of the ground-return mode is lower when frequency-dependent soil parameters are considered, as shown in Fig. 2. Consequently, the traveling voltage wave experiences reduced attenuation as it propagates along the cable, leading to higher voltage amplitudes, as discussed in the transient responses presented in Section IV.

Fig. 11 shows similar results but assumes a more realistic excitation, considering a voltage source with internal impedance $Z_S = 400\ \Omega$, which might be considered representative of the characteristic impedance of the overhead (OH) line. As observed previously, accounting for the frequency dependence of soil parameters in grounding modeling leads to a reduction in the resulting overvoltages at the cable sheath, especially for a poorly conducting soil. On the other hand, the influence of soil model on the cable characterization is not as significant as in the previous case. Some differences between the voltage waveforms are noted only in the first microseconds, especially for high-resistivity soils, as indicated in Figs. 11(b) and 11(c).

Another remarkable difference in comparison with the previous case, which assumed an ideal voltage source, is the reduced amplitude, the slower rise times, and the less oscillatory behavior observed in the voltage waveforms shown in Fig. 11. The first feature is explained by the voltage drop across the internal impedance of the source, which is nearly ten times larger than the characteristic impedance of the cable. The second one is caused by the filtering effect associated with the frequency response of the system seen at the connection point of the voltage source, which changes the rate of rise of the voltage applied at the cable end if $Z_S \neq 0$. Finally, the latter feature is related to the change in the voltage reflection coefficient at the sending end of the cable, which is -1 for $Z_S = 0$ and close to 0.8 for $Z_S = 400\ \Omega$.

Despite some simplifications, this case study emphasizes the importance of accurately modeling the underground section in lightning overvoltage simulations of mixed overhead-underground lines. This is particularly relevant when highly accurate results are required, as the frequency dependence of soil parameters has a significant impact on the computed overvoltages. Finally, it is important to note that the presence of surge arresters at the junction points may alter the voltage waveforms and their frequency content. This aspect will be investigated in future studies.

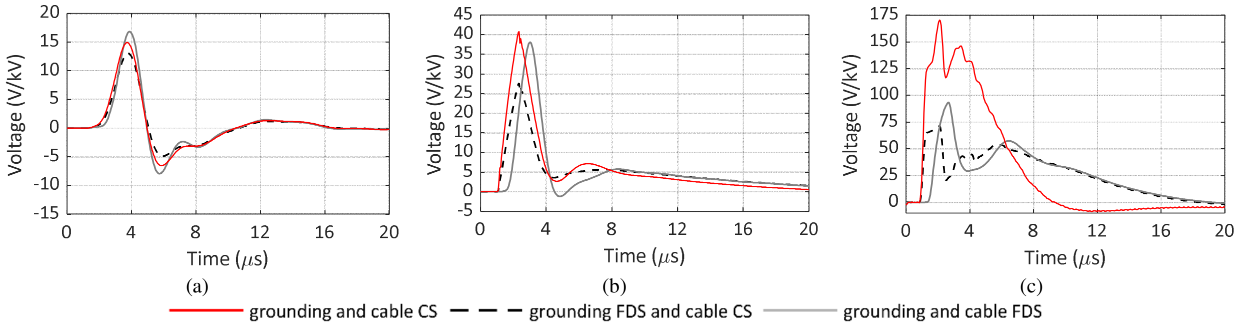

Fig. 10. Sheath voltage waveforms calculated at the receiving end of phase C for the application of a standard lightning impulse voltage (1 kV, 1.2/50 μs) to the sending end of the core of phase A, considering different soil resistivities: (a) 200 Ωm, (b) 1000 Ωm and (c) 5000 Ωm.

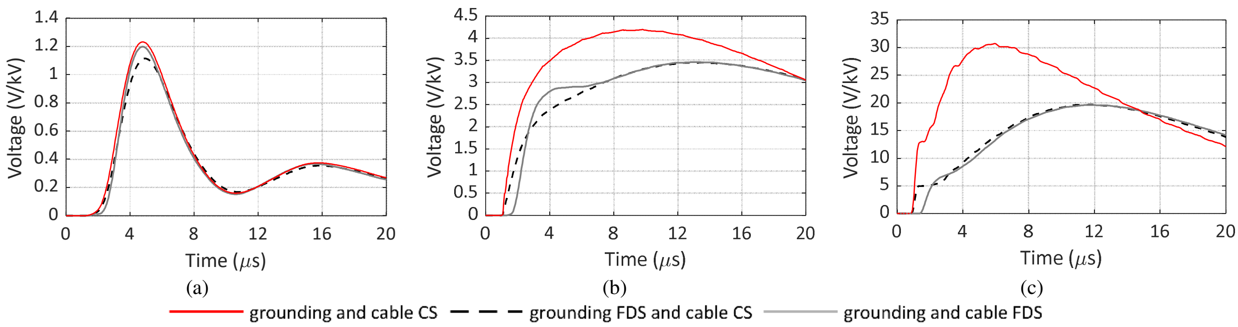

Fig. 11. Same as Fig. 11, but considering a series impedance $Z_S = 400\ \Omega$ with the surge voltage source in Fig. 8.

B. Ground Potential Rise in Wind Turbines Due to Direct Lightning Strikes

The open installation sites of wind farms and the increasing height of modern wind turbines (WTs) make these structures highly susceptible to direct lightning strikes. Wind farms typically consist of multiple turbines operating in proximity, with a separation approximately equal to the diameter of the rotor blades. The grounding systems of individual wind turbines are usually interconnected through buried bare conductors or the sheaths of insulated power cables. When a WT is struck by lightning, the resulting current is directed to the grounding system and dissipated into the earth, causing a ground potential rise (GPR). This GPR can damage or disrupt sensitive electronic equipment. Moreover, the flow of lightning current through the sheaths of power cables has been reported to damage their insulating layers, potentially compromising the integrity of the cables and increasing the risk of system failures.

To assess the influence of the frequency dependence of soil parameters on cable modeling and the potential rise caused by a lightning strike to a wind turbine, the system shown in Fig.

12(a) is analyzed. This configuration consists of a pair of WT grounding systems—with geometry detailed in Fig. 12(b)—interconnected through the sheath of an insulated cable. For simplicity, a single cable is considered, with the same geometrical parameters indicated in Fig. 1(b), and both core ends are left open. A normalized 1-kA current pulse with a rise time of 1 μs that is representative of typical lightning currents striking wind turbines is injected into the left grounding system, and both the GPR at the struck WT and the transferred voltage to the adjacent WT are computed. In the simulations, the frequency-dependent impedance of the WT grounding systems, $Z_{WT}(j\omega)$, is modeled using an accurate electromagnetic approach [31,32].

Fig. 13 shows the simulated GPR at the left WT and the transferred voltage (TV) to the adjacent WT, for soil resistivities of 1000 Ωm and 5000 Ωm. By comparing the red and black dotted curves, it is observed that incorporating frequency-dependent soil parameters in grounding modeling leads to a decrease in both GPR and transferred voltage to the adjacent WT. This effect is due to the improvement in the performance of WT grounding systems when the frequency dependence of soil parameters is accounted for, as demonstrated in [32] through both experimental and simulated results.

Considering the influence of FD soil parameters on cable modeling (comparing the gray and black dotted curves), the results reveal that the GPR peak is higher when the frequency-dependent nature of soil parameters is ignored in cable modeling, especially for the 5000-Ωm soil. This can be attributed to the fact that the characteristic impedance of the cable's ground-return mode, assuming constant soil parameters, is higher than that computed using frequency-dependent soil parameters. Consequently, a smaller fraction of the injected current is diverted to the adjacent tower through the cable sheath when constant parameters are assumed, resulting in a larger portion directed into the grounding system, which in turn produces a higher GPR. For instance, the difference in GPR peak is approximately 16% for the 5000-Ω soil.

Regarding the transferred voltages, the opposite trend is observed: higher peak values occur when the frequency-dependent soil assumption is adopted in cable modeling. This result, which is more evident for the 5000-Ωm soil, is attributed to the smaller attenuation experienced by the traveling voltage wave as it propagates along the cable when frequency-dependent soil parameters are considered, as discussed previously in Section IV.

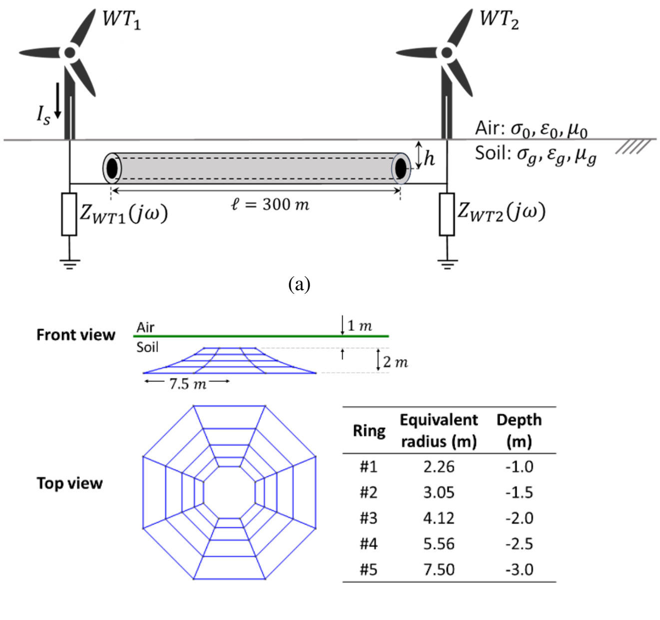

Ring	Equivalent radius (m)	Depth (m)
#1	2.26	-1.0
#2	3.05	-1.5
#3	4.12	-2.0
#4	5.56	-2.5
#5	7.50	-3.0

(b)

Fig. 12. (a) Representative system for simulating the GPR and transferred voltage (TV) in a wind turbine struck by lightning, and (b) WT grounding system geometry–Adapted from [33]

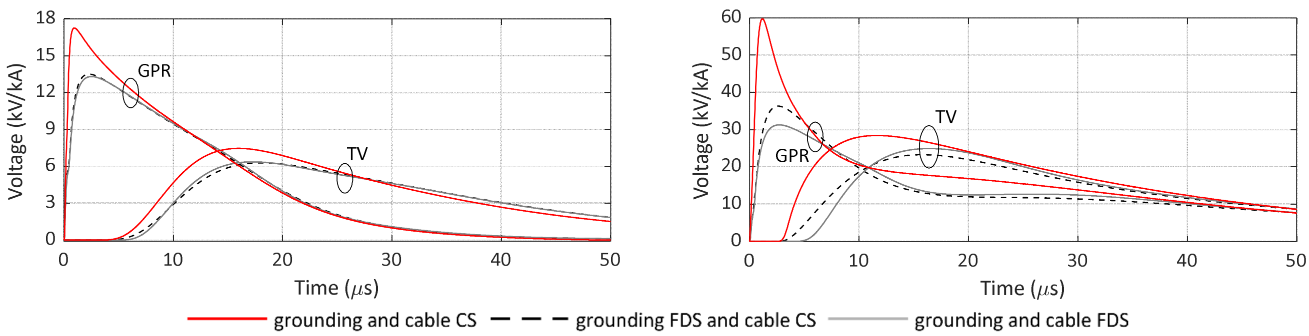

Fig. 13. GPR at the left WT and transferred voltage (TV) to the adjacent WT in the system depicted in Fig. 12(a), considering soil resistivities of (a) 1000 Ωm and (b) 5000 Ωm.

VI. Conclusions

This paper highlights the impact of the frequency dependence of soil parameters on the simulation of transient overvoltages in underground cables. The results indicate that this effect is particularly pronounced for short cables sections and poorly conducting soils, with resistivities higher than 1000 Ωm. In such cases, the frequency dependence of soil parameters leads to smaller attenuation of traveling waves and slower propagation velocities, resulting in noticeable differences in the simulated transient overvoltages when compared to models assuming constant soil parameters.

While the effect is more evident for high-resistivity soils and shorter underground cable sections, its magnitude may vary depending on the specific system configuration and type of transient phenomena under study, as demonstrated in the two case studies analyzed in this paper.

The findings presented in this article underscore the necessity of incorporating the frequency dependence of soil parameters in transient simulations of underground cables. It is expected that these results will inspire its inclusion in future studies and in commercial EMT-type simulation platforms, thereby enhancing the accuracy and reliability of transient analyses in practical applications.

VII. References

[1] T. A. Papadopoulos, D. A. Tsiamitros, and G. K. Papagiannis, “Impedances and Admittances of Underground Cables for the Homogeneous Earth Case,” *IEEE Transactions on Power Delivery*, vol. 25, no. 2, pp. 961–969, Apr. 2010.

[2] A. P. C. Magalhaes, J. C. L. V. Silva, A. C. S. Lima, and M. T. Correia de Barros, “Validation Limits of Quasi-TEM Approximation for Buried Bare and Insulated Cables,” *IEEE Trans Electromagn Compat*, vol. 57, no. 6, pp. 1690–1697, Dec. 2015.

[3] A. P. C. Magalhaes, M. T. C. de Barros, and A. C. S. Lima, “Earth Return Admittance Effect on Underground Cable System Modeling,” *IEEE Transactions on Power Delivery*, vol. 33, no. 2, pp. 662–670, Apr. 2018.

[4] H. Xue, A. Ametani, J. Mahseredjian, and I. Kocar, “Generalized Formulation of Earth-Return Impedance/Admittance and Surge Analysis on Underground Cables,” *IEEE Transactions on Power Delivery*, vol. 33, no. 6, pp. 2654–2663, Dec. 2018.

[5] N. Duarte, A. De Conti, and R. Alipio, “Extension of Vance’s closed-form approximation to calculate the ground admittance of multiconductor underground cable systems,” *Electric Power Systems Research*, vol. 196, p. 107252, Jul. 2021.

[6] A. De Conti, N. Duarte, and R. Alipio, “Closed-Form Expressions for the Calculation of the Ground-Return Impedance and Admittance of Underground Cables,” *IEEE Transactions on Power Delivery*, vol. 38, no. 4, pp. 2891–2900, 2023.

[7] A. De Conti, N. Duarte, R. Alipio, and O. E. S. Leal, “Small-argument analytical expressions for the calculation of the ground-return impedance and admittance of underground cables,” *Electric Power Systems Research*, vol. 220, p. 109299, Jul. 2023.

[8] N. Duarte, A. De Conti, and R. Alipio, “Assessment of Ground-Return Impedance and Admittance Equations for the Transient Analysis of Underground Cables Using a Full-Wave FDTD Method,” *IEEE Transactions on Power Delivery*, vol. 37, no. 5, pp. 3582–3589, 2022.

[9] N. Duarte, A. De Conti, R. Alipio, and F. Rachidi, “Assessment of the transmission line theory in the modeling of multiconductor underground cable systems for transient analysis using a full-wave FDTD method,” *Electric Power Systems Research*, vol. 223, p. 109570, Oct. 2023.

[10] W. G. B1.07, *Statistics of AC underground cables in Power networks*. CIGRE, 2007.

[11] T. V. Gomes, M. A. O. Schroeder, R. Alipio, A. C. S. de Lima, and A. Piantini, “Investigation of Overvoltages in HV Underground Sections Caused by Direct Strokes Considering the Frequency-Dependent Characteristics of Grounding,” *IEEE Trans Electromagn Compat*, vol. 60, no. 6, pp. 2002–2010, Dec. 2018.

[12] R. Tarko, J. Gajdzica, W. Nowak, and W. Szpyra, “Study of the Lightning Overvoltage Protection Effectiveness of High Voltage Mixed Overhead Cable Power Lines,” *Energies (Basel)*, vol. 14, no. 8, p. 2329, Apr. 2021.

[13] M. M. Osborne, A. Xemard, L. Prikler, and J. A. Martinez, “Points to consider regarding the insulation coordination of GIS substations with cable connections to overhead lines,” in *International Conference on Power Systems Transients (IPST’07)*, Lyon, 2007, pp. 1–5.

[14] Working Group C4.33, “CIGRE TB 781: Impact of soil-parameter frequency dependence on the response of grounding electrodes and on the lightning performance of electrical systems,” CIGRE, Paris, 2019.

[15] R. Alipio and S. Visacro, “Frequency Dependence of Soil Parameters: Effect on the Lightning Response of Grounding Electrodes,” *IEEE Trans Electromagn Compat*, vol. 55, no. 1, pp. 132–139, Feb. 2013.

[16] M. Akbari, K. Sheshyekani, and M. R. Alemi, “The Effect of Frequency Dependence of Soil Electrical Parameters on the Lightning Performance of Grounding Systems,” *IEEE Trans Electromagn Compat*, vol. 55, no. 4, pp. 739–746, Aug. 2013.

[17] M. Akbari *et al.*, “Evaluation of Lightning Electromagnetic Fields and Their Induced Voltages on Overhead Lines Considering the Frequency Dependence of Soil Electrical Parameters,” *IEEE Trans Electromagn Compat*, vol. 55, no. 6, pp. 1210–1219, Dec. 2013.

[18] F. H. Silveira, S. Visacro, R. Alipio, and A. De Conti, “Lightning-Induced Voltages Over Lossy Ground: The Effect of Frequency Dependence of Electrical Parameters of Soil,” *IEEE Trans Electromagn Compat*, vol. 56, no. 5, pp. 1129–1136, Oct. 2014.

[19] A. De Conti and M. P. S. Emídio, “Extension of a modal-domain transmission line model to include frequency-dependent ground parameters,” *Electric Power Systems Research*, vol. 138, pp. 120–130, 2016.

[20] R. Alipio, A. De Conti, A. S. de Miranda, and M. T. Correia de Barros, “Lightning Overvoltages Including Frequency-Dependent Soil Parameters in the Transmission Line Model,” in *International Conference on Power Systems Transients (IPST2019)*, Perpignan, 2019, pp. 1–6.

[21] H. Xue, A. Ametani, Y. Liu, and J. De Silva, “Effect of frequency-dependent soil parameters on wave propagation and transient behaviors of underground cables,” *International Journal of Electrical Power & Energy Systems*, vol. 122, p. 106163, Nov. 2020.

[22] T. A. Papadopoulos, Z. G. Datsios, A. I. Chrysochos, P. N. Mikropoulos, and G. K. Papagiannis, “Wave Propagation Characteristics and Electromagnetic Transient Analysis of Underground Cable Systems Considering Frequency-Dependent Soil Properties,” *IEEE Trans Electromagn Compat*, vol. 63, no. 1, pp. 259–267, Feb. 2021.

[23] N. Duarte, A. De Conti, and R. Alipio, “Transient Analysis of Buried Cables Considering a Nodal Admittance Matrix Approach,” in *2019 International Symposium on Lightning Protection (XV SIPDA)*, IEEE, Sep. 2019, pp. 1–6.

[24] T. A. Papadopoulos, Z. G. Datsios, A. I. Chrysochos, P. N. Mikropoulos, and G. K. Papagiannis, “Modal propagation characteristics and transient analysis of multiconductor cable systems buried in lossy dispersive soils,” *Electric Power Systems Research*, vol. 196, p. 107249, Jul. 2021.

[25] R. Alipio and S. Visacro, “Modeling the Frequency Dependence of Electrical Parameters of Soil,” *IEEE Trans Electromagn Compat*, vol. 56, no. 5, pp. 1163–1171, Oct. 2014.

[26] A. Ametani, “A General Formulation of Impedance and Admittance of Cables,” *IEEE Transactions on Power Apparatus and Systems*, vol. PAS-99, no. 3, pp. 902–910, May 1980.

[27] R. Alipio, N. Duarte, and F. Rachidi, “High-frequency transients in buried insulated wires: Transmission line simulations and experimental validation,” *Electric Power Systems Research*, vol. 237, p. 110993, Dec. 2024.

[28] J. A. Martinez-Velasco, *Power System Transients: Parameter Determination*. CRC Press, 2010.

[29] P. Moreno and A. Ramirez, “Implementation of the Numerical Laplace Transform: A Review Task Force on Frequency Domain Methods for EMT Studies, Working Group on Modeling and Analysis of System Transients Using Digital Simulation, General Systems Subcommittee, IEEE Power Engineering,” *IEEE Transactions on Power Delivery*, vol. 23, no. 4, pp. 2599–2609, Oct. 2008

[30] R. Alipio, H. Xue, and A. Ametani, “An accurate analysis of lightning overvoltages in mixed overhead-cable lines,” *Electric Power Systems Research*, vol. 194, p. 107052, May 2021.

[31] S. Visacro and A. Soares, “HEM: A Model for Simulation of Lightning-Related Engineering Problems,” *IEEE Transactions on Power Delivery*, vol. 20, no. 2, pp. 1206–1208, Apr. 2005.

[32] R. Alipio, D. Conceição, A. De Conti, K. Yamamoto, R. N. Dias, and S. Visacro, “A comprehensive analysis of the effect of frequency-dependent soil electrical parameters on the lightning response of wind-turbine grounding systems,” *Electric Power Systems Research*, vol. 175, p. 105927, Oct. 2019.

[33] R. Alipio, M. Guimarães, L. Passos, D. Conceição, and M. T. C. de Barros, “Ground Potential Rise in Wind Farms due to Direct Lightning,” *Electric Power Systems Research*, vol. 194, p. 107110, May 2021.